JOURNAL OF AIRCRAFT
Vol. 46, No. 3, May–June 2009

Vibration and Flutter Characteristics of a Folding Wing

Matthew P. Snyder*
U.S. Air Force Academy, Colorado Springs, Colorado 80840
Brian Sanders†
U.S. Air Force Research Laboratory, Wright–Patterson Air Force Base, Ohio 45433
and
Franklin E. Eastep‡ and Geoffrey J. Frank§
University of Dayton Research Institute, Dayton, Ohio 45469

DOI: 10.2514/1.34685

Studies are presented that characterize the dynamic aeroelastic aspects of a morphing aircraft design concept. The notion of interest is a folding wing design resulting in large-scale wing area changes. A finite element approach is used to investigate the sensitivity of natural frequencies and flutter instabilities to the wing position (e.g., fold angle), actuator stiffness, and vehicle weight. Sensitivities in these areas drive design requirements and raise flight envelope awareness issues. The study is presented in two parts as a comparison between two models of varying complexity. A simple folding wing model, based on the Goland wing, is analyzed and results are compared with a built-up structural model of the proposed full scale morphing vehicle.

Introduction

THE concept of wing shape control had its roots in the original flying machine. The Wright brothers used wing warping or twisting for roll control of the first flying machine. Varying the shape of the wing enabled the Wright brothers to control the roll of the aircraft. The evolution of aircraft, however, followed a path of fixed geometry, high stiffness wings. As a result, with a fixed wing configuration, air vehicles are optimized for specific flight conditions, for example, commercial airliners were designed to be aerodynamically efficient for cruising long distances at a set speed and altitude. Flight dynamists have long realized changes in wing configuration could provide significant increases in-flight efficiency. One example is swept wing technology where wing sweep changes with increasing speed resulting in an air vehicle with greater aerodynamic efficiency throughout its flight envelope. An unswept wing provides a balanced aerodynamic configuration at subsonic speeds, but sweeping the wing between 50 and 60 deg improves flight performance during supersonic cruise. In an effort to exploit the benefits of multiple configurations the variable swept wing was introduced. Figure 1 shows the U.S. Air Force B-1 bomber in its unswept and swept wing configurations.

Variable wing sweep design, however, contains limitations such as the shift in aerodynamic center which affects aircraft stability.

Another example of in-flight wing configuration change was incorporated in the folding mechanism of the XB-70 Valkyrie. The designers of the XB-70 Valkyrie engineered an out of plane wing folding mechanism for aerodynamic performance improvement. Figure 2 shows the wing in its three fold positions.

The wings remain in the horizontal configuration at speeds below 300 kt. From 300 kt to Mach 1.4 the wing tips were folded down 25 deg and at speeds greater than Mach 1.4 the wing tips were folded to 65 deg. This wing folding resulted in three distinct aerodynamic advantages. The increased vertical area allowed shorter vertical stabilizers to be used. Secondly, the wing folding offset the rearward shift in center of lift with increasing speed of the delta wing, in turn reducing drag-inducing trim corrections. Finally, it enabled better management of compression lift, or the lift gained due to the increase in surface pressure on the underside of the wing, increasing lift effectiveness by 30% [1].

These examples of wing area change, however, drive towards increasing performance of a vehicle designed for a single mission. A different approach is to examine wing area change in a vehicle designed for multiple missions and increased single mission efficiency. Currently, an air vehicle is mission length and performance limited by wings designed for set flight conditions, cruise, loiter, and engagement.

In an effort to exploit this concept, the Defense Advanced Research Projects Agency Morphing Aircraft Structures program is developing novel technology defined by the goal of using radical wing shape changes to expand the flight envelopes and operational characteristics of flight vehicles. Morphing vehicles are classified as structures exploiting actuation mechanisms to achieve substantial wing area change resulting in previously unachievable performance as demonstrated through interaction with diverse mission requirements. This involves the development and integration of advanced materials, actuation systems, mechanisms, and control laws. The concept behind morphing vehicles stems from the desire to expand mission capabilities of aircraft platforms. Radical wing area changes enable a single air vehicle to perform a variety of tasks normally involving multiple aircraft with varying missions. In this coming age of unmanned aerial vehicles human induced flight termination is replaced by vehicle limitations such as range and engine performance. A morphing vehicle will expand the range of a vehicle by increasing its mission segment efficiency. For example, the vehicle could cruise at an optimal configuration and then morph into an optimal dash or loiter configuration.

Limitations exist due to structural design considerations, aeroelastic instabilities limiting the flight envelope, lack of actuator power for driving such designs, or skins not able to withstand strains imposed by actuation. The radical changes in wing area described in this paper are the synthesis of new materials, designs and flexible structural components capable of maintaining aerodynamic shape while varying structural configuration. A concept which achieves a 200% wing area change is the Lockheed Martin folding wing aircraft, shown in Fig. 3 illustrating the vehicle morphing from a cruise to high-speed dash configuration.

Previous research [2] explains how the inclusion of a flexible wing fold hinge and sweeping of that hinge line can enhance performance characteristics, similar to aeroelastic tailoring. However, this folding

Received 19 September 2007; accepted for publication 12 February 2009.

*Assistant Professor of Engineering Mechanics. Member AIAA.
†Senior Aerospace Engineer, Building 146, 2210 8th Street. Associate Fellow AIAA.
‡Emeritus Professor, 300 College Park Avenue. Fellow AIAA.
§Senior Research Engineer, 300 College Park Avenue. Member AIAA.

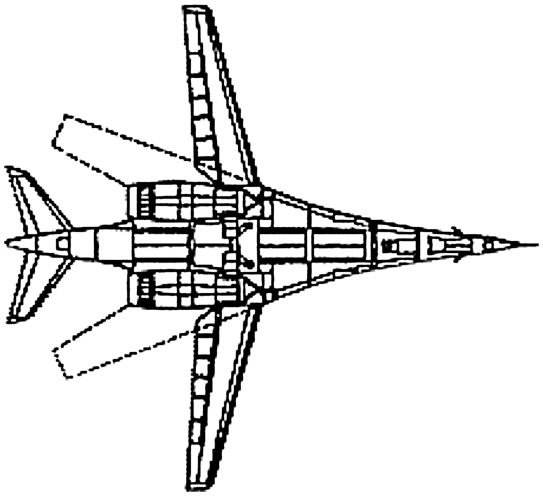

Fig. 1 B-1 Lancer swept wing.

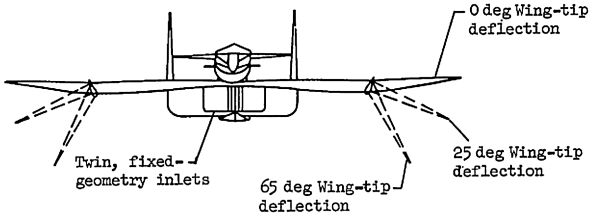

Fig. 2 Wing folding as demonstrated by the XB-70 [7].

Fig. 3 Lockheed Martin morphing vehicle [8].

wing concept extends to the next level by folding the entire wing structure against the fuselage to radically reduce wing area as necessary for flight envelope expansion and improved performance. The change in wing area comes from two chordwise wing folds, one at the wing root and the other at approximately 30% span. The wing folds are driven relative to each other, the inner wing rotates approximately 130 deg from the unfolded to the folded configuration while the outer wing remains in a horizontal orientation. Flexible skins at the joints maintain the aerodynamic shape as the wing folds. Shape control of the leading edge of the inner wing forces it to conform to the fuselage in the fully folded condition. The vast change in area enables mission planners to design unique mission profiles to take advantage of the characteristics of the flight vehicle.

The in-flight changes in configuration, driven by the integration of newly developed structural, material, and actuator technologies, result in some unique aeroelastic considerations [3]. Modal frequencies will be changed by the folding of the wing and the flutter mechanism will vary as the modes couple and uncouple throughout the fold angle range. The study of the full scale folding wing concept [4] is undertaken simultaneously with the analysis of a simple folding wing [5]. The simple folding wing is a beam-rod model of the Goland wing [6] modified to include folding springs at the root and 40% semispan. Because of the complexity of the built-up structural model, results from the simplified analysis are used to identify trends that can be used to interpret changes in modal and flutter analysis data obtained from the built-up model. Aeroelastic data from finite element models of the beam-rod model wing and built-up folding wing is used to find folding wing unique aeroelastic properties and then presented for analysis and conclusion.

Problem Definition

The built-up structural model is quite complex therefore clouding the results of the aeroelastic analysis. In an effort to determine how folding and unfolding the wing affects aeroelastic properties a simplified model is introduced. The single spar Goland wing model is used to identify aeroelastic trends associated with the folding wing. The model consists of a single spar represented by beam elements two feet in length and located at the elastic axis. The wing has a span of 20 ft and a chord of 6 ft, which is defined by an aerodynamic grid. A representation of the model is shown in Fig. 4.

The beam-rod wing model is modified to resemble the built-up finite element model as the wing is broken into two wing sections joined by a spring element representing the actuator mechanism. A root spring models the root actuator. The actuators are positioned at the wing folds and represent a rotary actuation system which would carry the applied air loads and actuation loads. In addition to the elastic elements, rigid bars are added to aid in the visualization of torsion modes. Figure 5 illustrates the simple fold model.

The wing is shown at a 45 deg wing fold angle in Fig. 6. The root spring drives the inner wing to rotate while the outer spring maintains the outer wing in a horizontal configuration. The initial spring constant of both fold springs is determined by dividing the Goland wing bending stiffness by twice the semispan.

Quasi-steady folding motion is assumed based on the length of time, estimated to be 1 min or more, for wing folding from the fully unfolded to folded configuration. Flutter characteristics over the range of fold angles are obtained by varying the wing fold angle by 5 deg increments. Modal and flutter analyses results are obtained as a function of variation in fold spring stiffness and wing fold angle. Flutter results are obtained at several orders of magnitude above and below the initial spring stiffness values. Here the wing fold angles vary from 0 deg, the fully unfolded configuration, to 90 deg.

In similar fashion a semispan model (i.e., half fuselage and one wing) of the Lockheed Martin model is considered at various wing fold angles. The following, Fig. 7, shows the model at a 45 deg angle. Note the fully folded configuration results in an inner wing fold angle of 130 deg.

The model contains three main sections: an inner wing, outer wing, and fuselage. The two wing sections are joined to each other and the fuselage by elastic elements with specified stiffness to

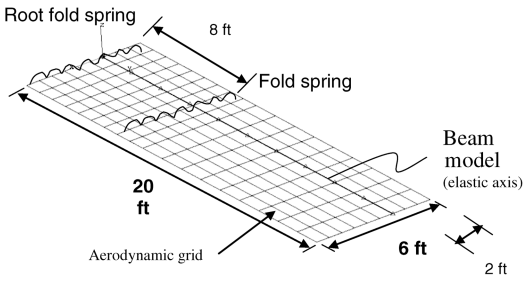

Fig. 4 Goland wing beam model.

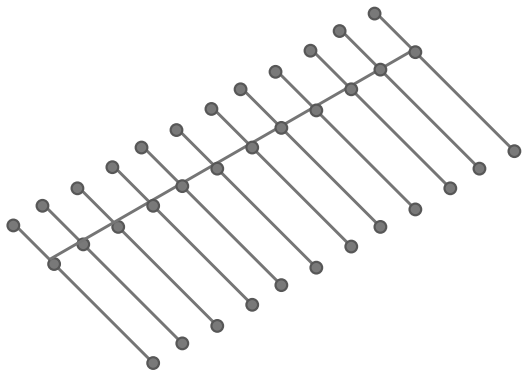

Fig. 5 Goland wing beam-rod finite element model.

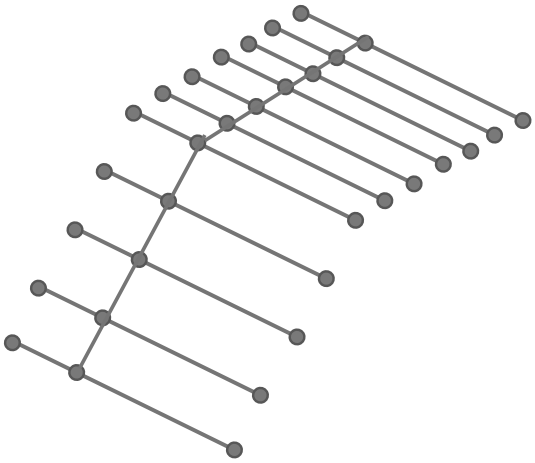

Fig. 6 Goland folding wing, shown at 45 deg wing fold angle.

Fig. 7 Lockheed Wing shown at 45 deg fold angle.

represent the actuator mechanisms. The elastic elements allow rotation about an axis in the chord wise direction of the wing. As the wing folds these elements provide all of the stiffness in this direction and carry all associated air and structural loads. There are leading and trailing edge control surfaces on the inner wing in addition to an elevon on the outer wing. Composed of 5134 elements the 11,500-degree-of-freedom model has been structurally optimized for the expected air loads. The aerodynamic models used for vibration and flutter analysis are NASTRAN flat-panel, doublet lattice models. Loads and displacements are transferred to the FEM through infinite plate splines. The aircraft is modeled in free flight with appropriate boundary conditions applied for symmetric and antisymmetric conditions. Figure 8, a top down view, illustrates the finite element structural representation of the finite element model.

Modal and flutter results are obtained at several different actuator stiffnesses, vehicle weights, and wing fold angles. The initial stiffness of the actuator hinge elements is roughly based on the stiffness of the leading edge control surface of a typical U.S. Air Force fighter vehicle. Flutter results are obtained at 10, 50, and 75% of those initial values. Reduction in stiffness is a concern as one actuator concept involves a 1 order of magnitude drop in resistance during operation. However, once the desired wing fold angle is obtained, the stiffness of the mechanism returns to the original value. This illustrates the importance of understanding how advanced materials may impact the vehicle.

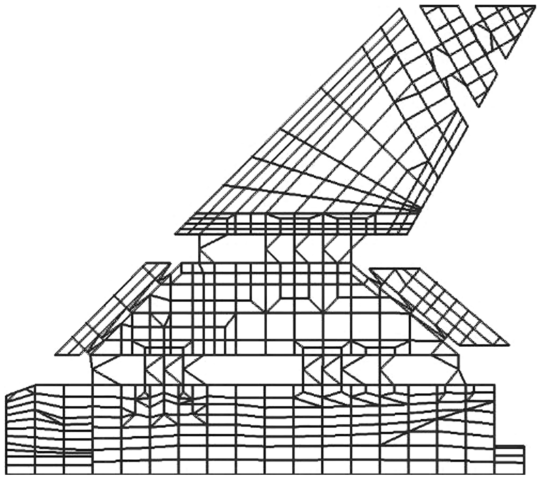

Fig. 8 Finite element model illustration.

The wing fold angle varies at 15 deg increments from 0 deg, fully unfolded configuration, to 130 deg, fully folded and latched configuration. Results are obtained for two vehicle weights, takeoff gross weight (TOGW) and fuel empty weight configurations.

Results

Modal Analysis

Modal frequencies are obtained for each fold angle and hinge stiffness. These frequencies are obtained from MSC NASTRAN using the Lanczos eigenextraction method and MSC PATRAN is used for visualization. The first ten modes were obtained; however, flutter results show that only the first four modes play a significant role in the results. Figure 9 shows the mode shapes of the first four modes at a wing fold angle of 45 deg. The figure is meant only to show the shape of the modes, frequency values change with hinge stiffness.

These four modes, two spring modes and two torsion modes, play a prominent role in the flutter analysis. Sp1 and Sp2 are the two spring modes, while tin and tout are the torsion modes. Sp1 denotes the root spring mode which resembles a first bend mode. Sp2 is the mode associated with the rotation of the joint at the spring connecting the wing sections. Tin refers to torsion of the inner wing section. Depending on fold angle this motion causes the outer wing to twist or have a lateral fore-aft sweeping motion. Tout represents torsion of the outer section and in most cases the inner section of the wing remains relatively stationary as the tout mode is excited.

Mode frequency and shape data is collected for varying wing fold angles at stiffnesses 1 order of magnitude either above or below that of the initial value. The effect of fold angle on modal frequency is plotted in Fig. 10 for the baseline spring stiffness, the case where the hinge stiffness is equal to the structural stiffness.

Modal frequency is plotted as a function of wing fold angle to illustrate frequency changes throughout the range of folding motion. Initially frequencies were obtained at 15 deg increments, but narrower 5 deg increments were used around areas of interest. Between 0 and 15 deg it should be noted that 1) there is a large decrease in frequency of the mode designated tout, and 2) tout crosses the Sp2 mode. The drop in frequency is explained by changing mode shapes resulting from wing folding. The crossover that occurs, also observed between 40 and 45 deg between Sp1 and tin, reflects a structural mode change.

While the crossing of the tout and Sp2 modes is clearly a mode change it is more difficult to distinguish between the Sp1 and tin modes. The modes do cross, but the exact crossing point is hard to distinguish. As the modes grow closer in frequency, reference the Sp1 and tin modes in the above plot at 30 deg, the mode shapes begin to take on characteristics of the other shape. The bending becomes a combination of spring and torsion modes and makes it difficult to ascertain the exact point where the modes actually cross. Whether or not these modes cross is not significant, the significance lies in the fact that their interaction causes the flutter mechanism to change.

Modal frequencies similar to that shown in Fig. 10 were gathered for hinge stiffness values designated by e4, e5, e7, e8, and e9. There is no difference between the cases designated e8 and e9, the case was run to ensure the stiffness of the springs had greatly exceeded that of the structure. Figure 11 shows the modal frequencies for two cases, in one case the hinge stiffness is less than the baseline stiffness, in the other it is greater.

From these plots some interesting observations emerge. The crossing that was discussed for the e6 case takes place only when the hinge stiffness value is equal to or greater than the initial stiffness

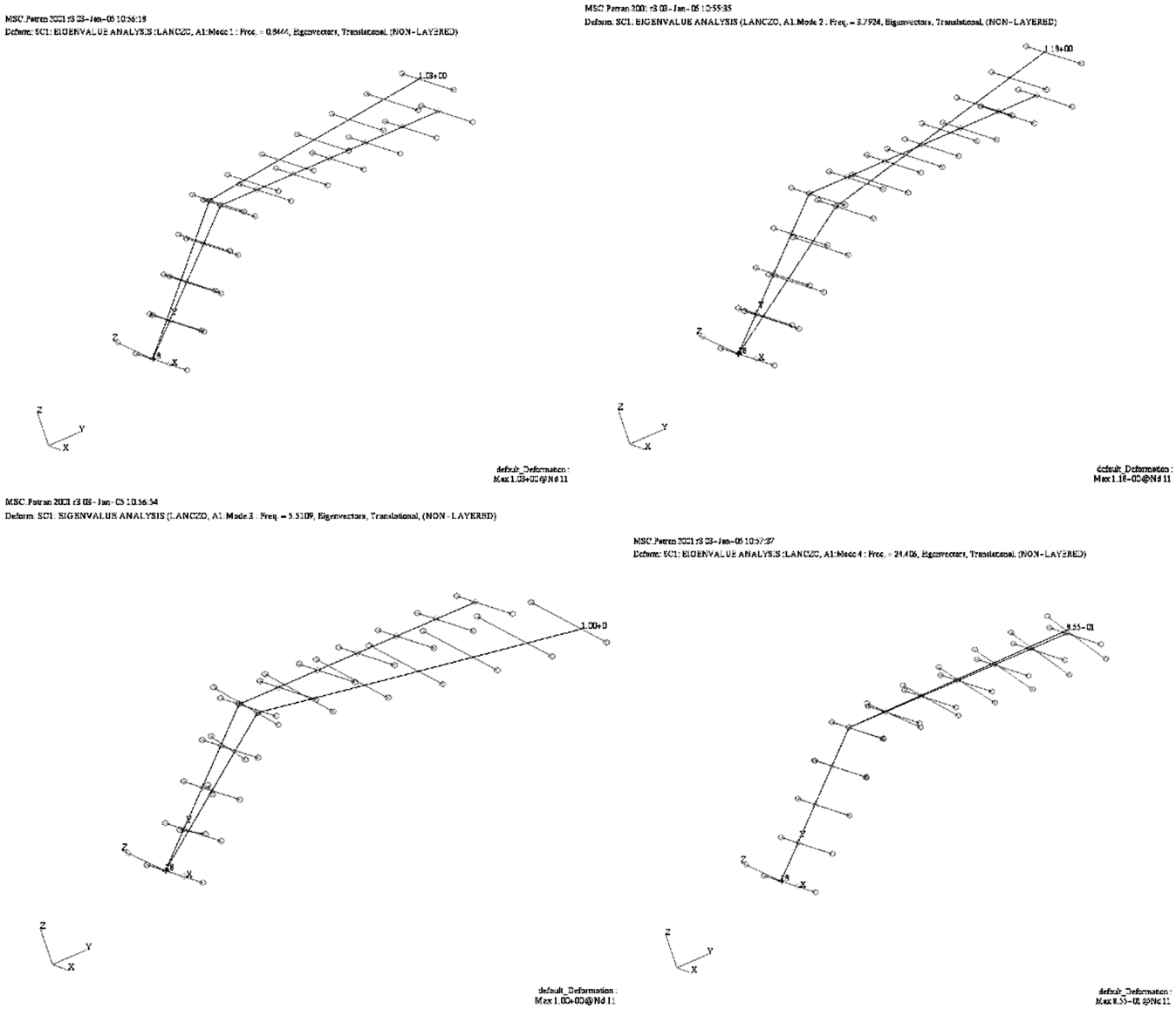

Fig. 9 Four modes of Goland folding wing; top left: Sp1, top right: Sp2, bottom left: tin, bottom right: tout.

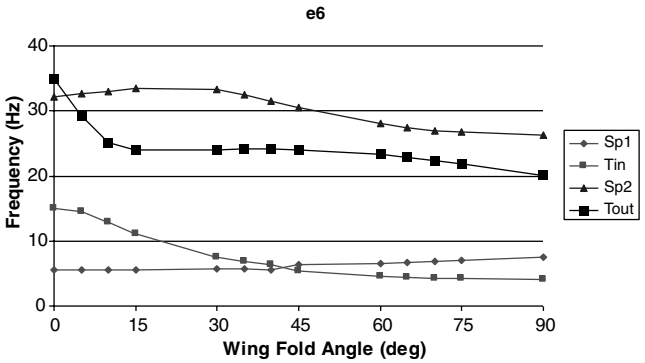

Fig. 10 Plot of Goland wing modal analysis results, initial hinge stiffness, that is, e [4].

value. The frequency values of the Tin and Tout modes do not change at different hinge stiffness values. The spring modes do change in frequency as a function of hinge stiffness. This is expected as stiffness is only provided in the direction of bending by the elastic elements. The Sp1 mode remains fairly linear over the range of hinge stiffnesses, with the exception of the mode switching that takes place. However, there is a large variation in the Sp2 mode. The frequency of this mode dramatically increases as the hinge stiffness magnitude increases.

Having concluded a trend study with the Goland wing model analysis of the built-up structural model is undertaken. The Goland wing results are compared with those of the high complexity model. When analyzing the built-up model, data from the first 40 modes were obtained; however, the majority of those modes are local modes, that is, modes dominated by deformation of a single small panel. Mixed among the local modes are the global modes, modes where deformation occurs in a large part of the structure, that are of interest. Mode shapes, derived from MSC PATRAN, are shown in Fig. 12. The figures only represent mode shapes, the frequency values change when the stiffness is adjusted.

The first and second bending modes are the typical bending modes. For the two fuselage bend modes bending occurs along the length of the fuselage which in turn causes either wing bending or wing torsion. In one case the fuselage bend leads to a wing torsion mode, in the other wing bending. Two torsion modes are seen, one is an inner wing torsion that, as the wing fold angle increases, drives a lateral sweeping motion in the outer wing. The second is torsion of the outer wing, which when excited generates little to no response in the inner wing. Visualizations, such as Fig. 12, determined how individual modes changed as a function of variations in hinge stiffness, wing fold angle, and aircraft weight. For specified vehicle

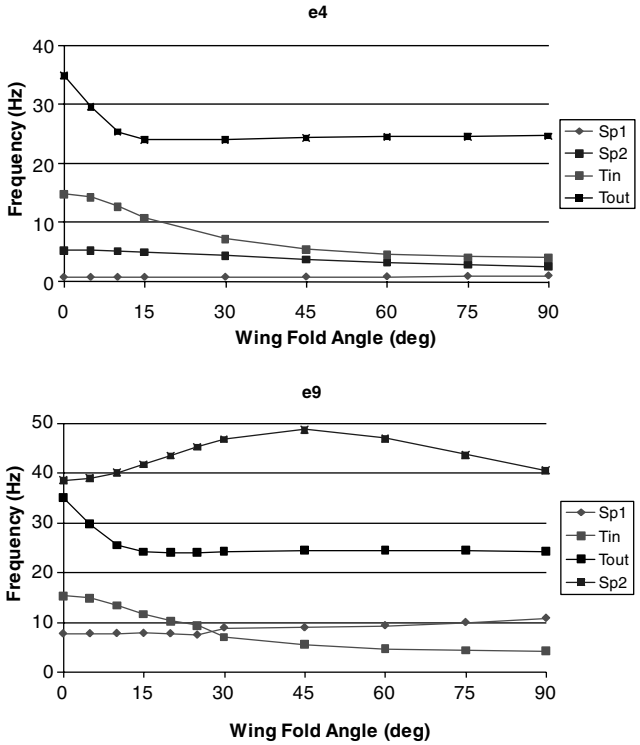

Fig. 11 Goland wing modal analysis results, other hinge stiffness values.

weight and hinge stiffness, plots were created to aid in data interpretation.

A plot of the modal frequency variation obtained for the baseline stiffness is shown in Fig. 13. Data was taken assuming the aircraft to be at TOGW.

1B represents the first bending mode, 2B the second bending mode, FBT designates fuselage bending driving wing torsion, FBB designates fuselage bending driving wind bending, tin is the torsion of the inner wing section and Tout represents torsion of the outer wing section. The horizontal axis is various fold angles between 0 and 130 deg with data taken in 15 deg increments. The first bending mode remains fairly constant in frequency throughout the range of fold angles and does not seem to couple with other modes. This seems to be true as well for the FBB and tout modes. There is a drop, however, in the frequency of the second bending mode. It appears to couple with either the FBT or tin mode between 45 and 60 deg before once again separating. The FBT and tin modes are items of interest due to the apparent mode switch that occurs between 45 and 60 deg. There is remarkable similarity between the two modes. At the 0 deg fold angle there are subtle differences in the mode shapes that allow one to distinguish between them. The tin mode is a pure torsion mode and the displacement of the wing tip is larger than the torsional displacement driven by the fuselage bending in the FBT mode. Likewise in the FBT mode the amount of bend in the fuselage is greater than that of the bending in the tin mode. As the fold angle increases it is increasingly difficult to tell the modes apart simply based on the mode shape visualizations. Whether or not the modes do switch the important characteristic to note is the interactions and coalescence, which play significant roles in the flutter results.

The symmetric and antisymmetric modes are compared in Fig. 14. As expected, they compare rather well. The fuselage bend modes exist only for the symmetric motion and are not shown on the plot.

Additional plots were obtained as hinge stiffness and weight varied. The ensuing plots show differences between the baseline case, initial stiffness and TOGW, for the sake of comparison and discussion. Figure 15 highlights differences between the baseline hinge stiffness and half hinge stiffness.

As expected, as a general trend, the frequencies of the modes from the half-stiffness analysis are lower than those of the baseline stiffness. There are a couple of interesting observations. The tout mode for the lower stiffness has a higher frequency at the 0 and 15 deg fold angle cases than the higher stiffness modes. Also, the mode switching seen in the higher stiffness case does not occur in the lower stiffness. As explained above, the mode switching was structural not numerical. While this may not seem to be the case after reviewing the lower stiffness data, it is seen that the modal coupling that took place during the higher stiffness case is not as influential in the lower stiffness study. It is very likely, then, that the switching would not take place in the lower stiffness case as the modal coupling is not as strong.

Not only was the stiffness reduced by 50% but there was also a case run where stiffness is reduced by an order of magnitude, shown in Fig. 16.

The results are as expected, the less stiff wing has lower frequencies associated with the global modes. It is surprising that there is mode switching in this case as there is clearly even less modal coupling than in the half-stiffness case.

A final series of modal frequency results are obtained to determine the effect of vehicle weight on frequency. Results from the TOGW configuration are compared with an empty weight configuration for baseline hinge stiffness in Fig. 17.

The above results show that weight decreases the frequency of modes. As seen in the plot the frequencies of the empty vehicle are greater than those of the vehicle at TOGW. Once again it is interesting to note the mode switching between the tin and FBT modes does not occur.

Flutter Analysis

The PK method is used to obtain flutter solutions for the folding Goland wing and Lockheed Martin wing for hinge stiffness values and wing fold angles shown in the preceding section. Flutter speeds are obtained and plotted from the ensuing V-g and V-f curves. The following plot, Fig. 18, demonstrates the appearance of a typical V-g, V-f diagram.

This plot contains data from the baseline hinge stiffness case, where hinge stiffness is of the same order of magnitude as that of the structure, and results are shown for the 0 deg wing fold angle. Mode 2, which is the inner torsion mode, is the flutter mode as seen by the crossing in the V-f diagram. It coalesces with the first bend mode driving the flutter crossing. As seen in Fig. 18, torsion of the inner section is the primary flutter mechanism in every case, with a few exceptions at high spring stiffness and greater fold angles.

Figure 19 is a depiction of flutter speed as a function of wing fold angle. Results are shown for each of the spring stiffness values which were studied.

Several interesting observations can be made from this figure. The two lines, which start above 600 ft/s at 0 deg fold angle and display linear behavior, are the cases where the two hinge stiffness values are less than that of the structure. At a hinge stiffness value of e6 there is a minimum in the flutter velocity at a 35 deg wing fold angle and flutter speed drastically increases before eventually leveling off. This low point, or bucket, in the results corresponds to the point where the mode crossing or interaction of the first spring and inner torsion modes takes place, as shown in the modal frequency results. All the cases where the values of hinge stiffness were greater than those of the structure also contain this "bucket," likewise corresponding to the crossing seen in the modal frequency results. The circled region shows the points at which the flutter mechanism changes. The flutter mechanism is torsion of the inner section outside the circled region and torsion of the outer section inside the circled region. The flutter frequencies increase as the flutter velocities increase and this can be seen in Fig. 20. Large jumps in the flutter frequency correspond to jumps in flutter velocity. It is interesting to note that the jump in flutter frequency lags that of the flutter velocity. For instance, in the hinge stiffness case of e6 the minimum is at 35 deg, however, the flutter frequency does not increase until 65 deg.

Having completed a modal analysis study of the Lockheed-Martin folding wing attention is turned to the study of flutter phenomena. Using the PK method in MSC NASTRAN, tables of V-g and V-ω;

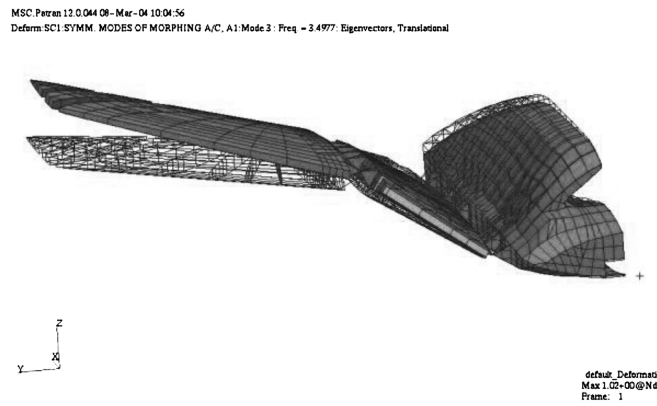

a) First bending

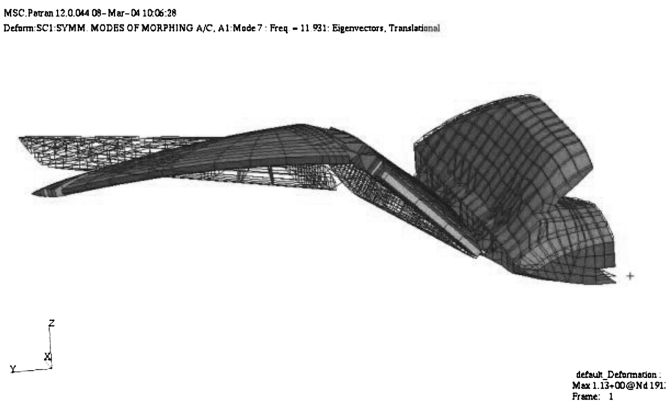

b) Second bending

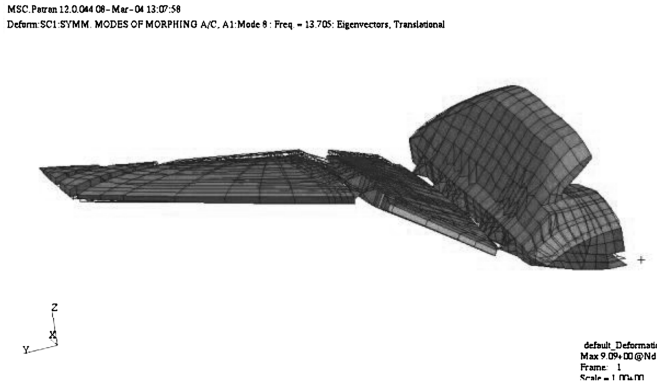

c) Fuselage bend with wing bending

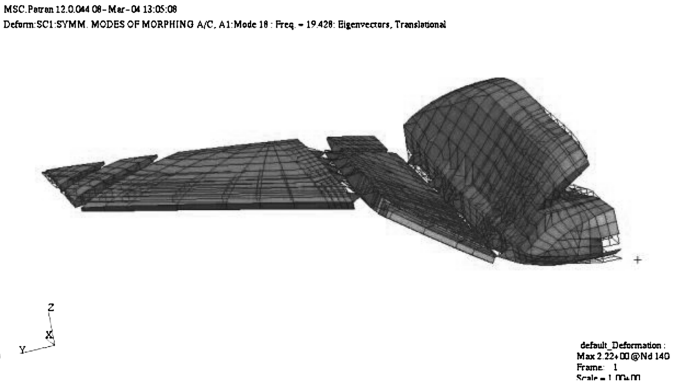

d) Fuselage bend with wing torsion

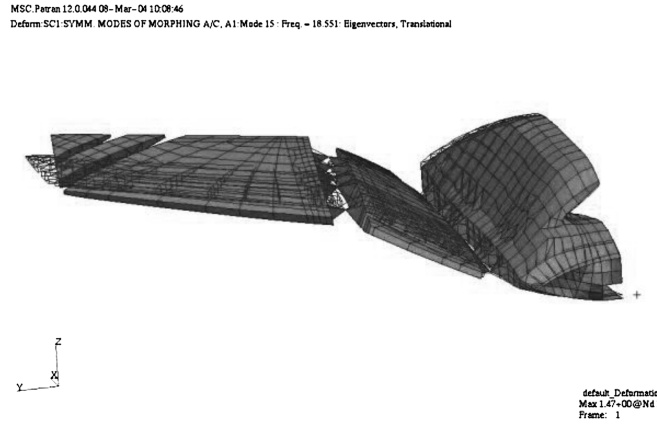

e) Torsion of inner wing section

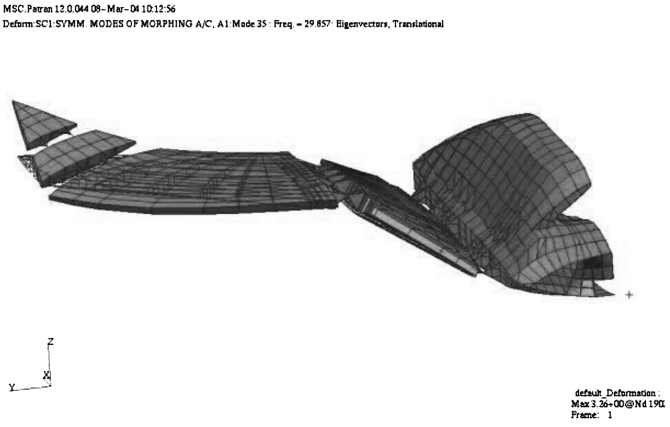

f) Torsion of outer wing section

Fig. 12 Lockheed wing mode shapes.

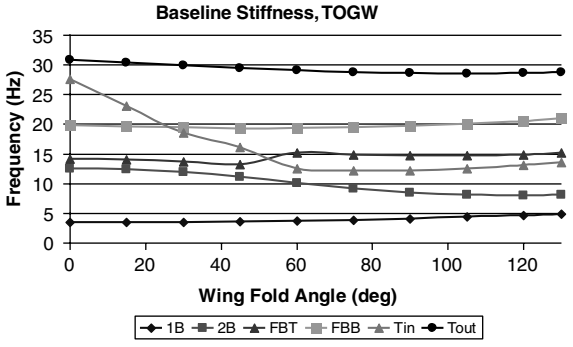

Fig. 13 Plot of modal analysis results.

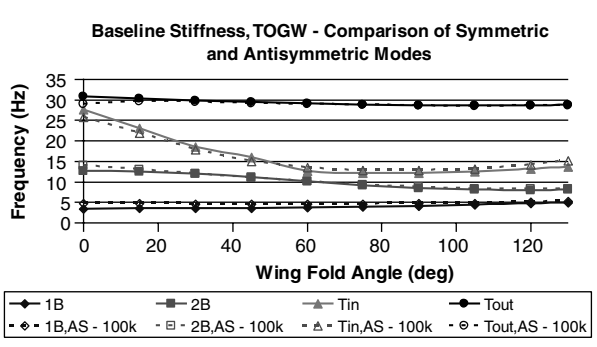

Fig. 14 Symmetric and antisymmetric mode comparison.

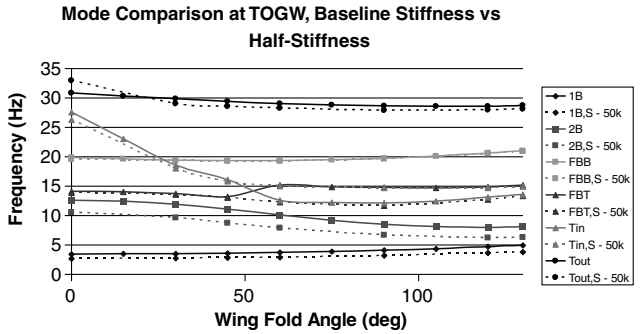

Fig. 15 Mode comparison, baseline and half hinge stiffness.

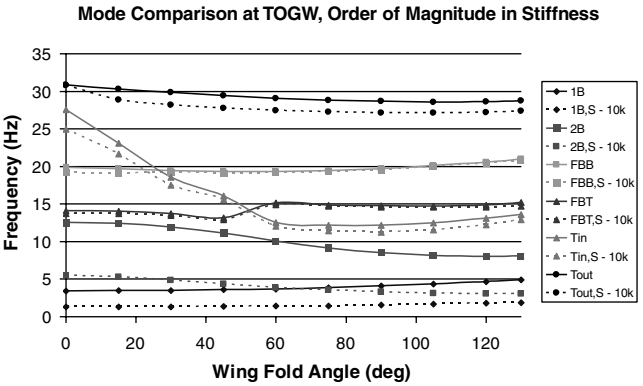

Fig. 16 Mode comparison, order of magnitude difference in stiffness.

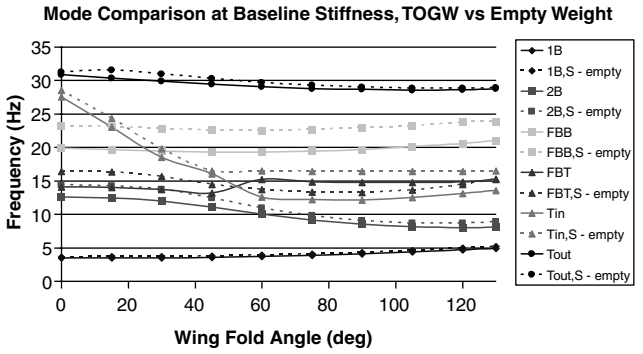

Fig. 17 Mode comparison, TOGW vs empty weight.

data were generated, and plotted for comparison. Figure 21 is the plot for the baseline hinge stiffness, TOGW, 0 deg fold angle case.

Similar plots were generated at 30 deg fold angle intervals for each configuration. Flutter speeds identified from the V-g and V-ω plots are summarized in Fig. 22.

Figure 22 shows flutter results for four stiffness configurations at TOGW. Following a line style, such as dashed, indicates a particular hinge stiffness while the marker symbol is indicative of the flutter mode. From the plot it is seen the flutter mode when the wing as folded to 90 deg was body freedom flutter for each hinge stiffness. For instance, the dotted line indicates flutter speeds in the baseline hinge stiffness configuration. As a function of fold angle and hinge stiffness flutter speed varies quite significantly and the flutter mode changes as well. Comparing this plot with the results generated in the modal analysis explains these results. The flutter mode in the 0 deg wing fold angle is the second bend mode. Looking at the modal analysis results it is seen the second bend mode couples with the fuselage bend/wing torsion mode, likewise at the 30 deg wing fold angle case. However, at 60 deg the flutter mode changes to Tin. This change occurs after the mode switching seen in the modal analysis. At 90 deg, the flutter mode changes again, this time to body freedom

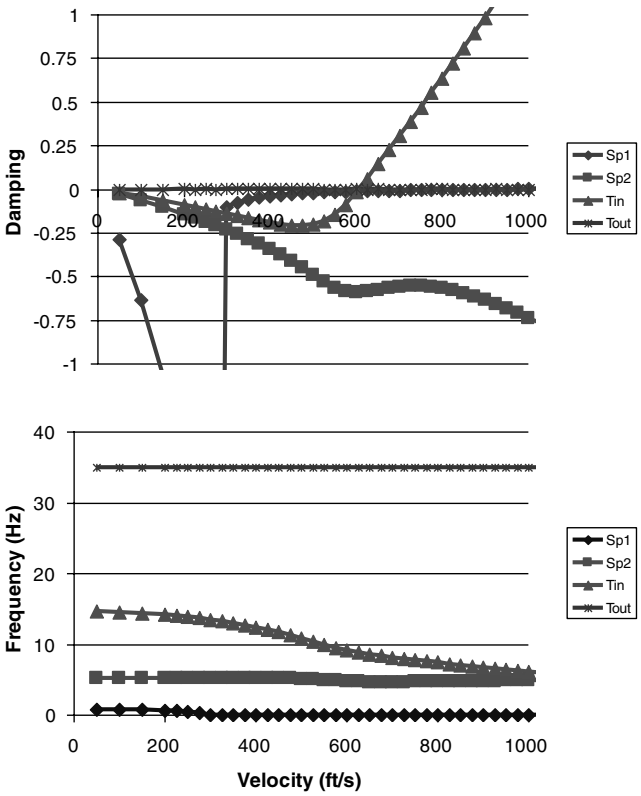

Fig. 18 Goland wing V-f, V-g diagram, e6, 0 deg fold angle.

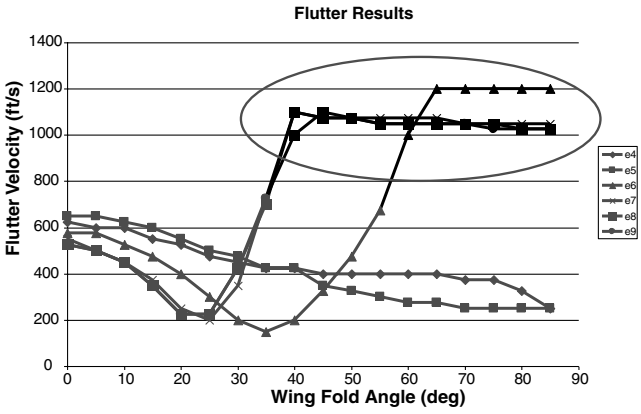

Fig. 19 Goland wing flutter velocity as a function of fold angle and hinge stiffness.

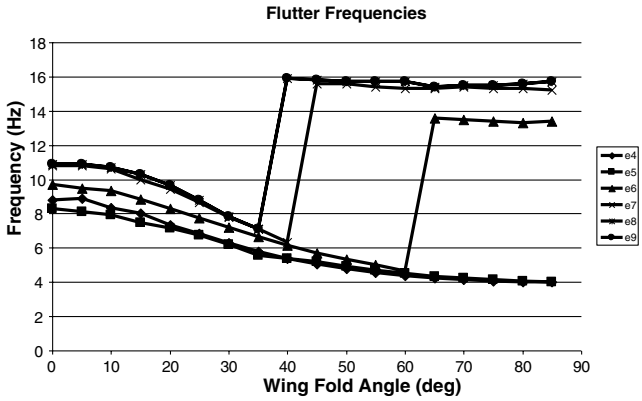

Fig. 20 Goland wing flutter frequency as a function of fold angle and hinge stiffness.

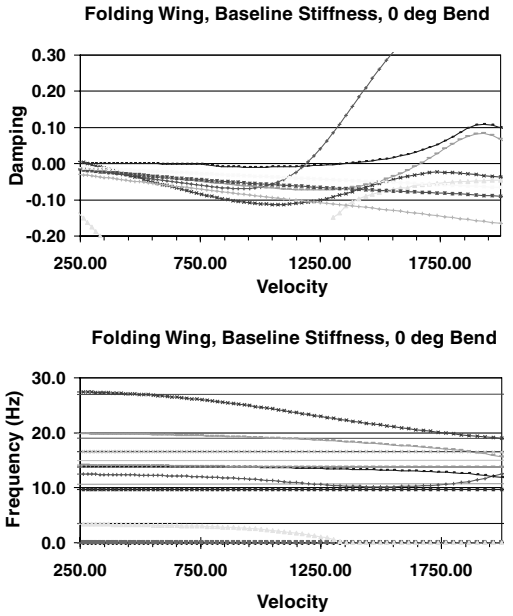

Fig. 21 Lockheed wing *V-g*, *V-ω* plots, baseline hinge stiffness, TOGW, 0 deg fold angle.

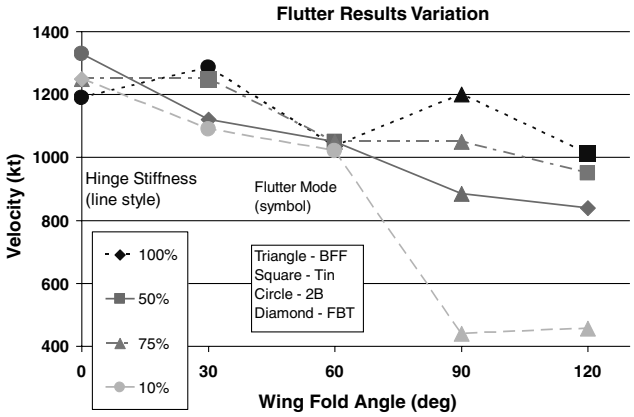

Fig. 22 Lockheed wing flutter analysis results, TOGW.

flutter which is the condition that occurs when the first bend mode couples with the short period mode. In the 90 and 120 deg wing fold angle cases, for a stiffness reduced by 1 order of magnitude, it is seen flutter speeds drop significantly. Other flutter mode switches can be traced in a similar fashion.

A comparative investigation was conducted for the empty weight configuration. The results are presented in Table 1.

Table 1 Flutter results for empty weight configuration

Baseline stiffness		
Wing bend angle, deg	Flutter velocity	Mode
0	860	BFF
30	840	BFF
60	885	BFF
90	1000	BFF
120	930	FBT
10% hinge stiffness		
Wing bend angle, deg	Flutter velocity	Mode
0	330	BFF
30	300	BFF
60	315	BFF
90	350	BFF
120	400	BFF

As seen from Table 1 the flutter velocities are much lower, all within the flight envelope, and all display body freedom flutter as the flutter mode.

Conclusions

Analysis of both the Goland wing model and the built-up structural model demonstrates the aeroelastic characteristics associated with folding the wing. The trends observed during Goland wing analysis are used to interpret trends seen in the complex model. The data shows there is a strong interrelationship between fold angle and hinge stiffness in regards to the modal and flutter analyses. The modal analysis shows bending modes are greatly impacted by changing the hinge stiffness. This result is expected as the modeled hinges carry the entire load across the joined sections. The single unconstrained degree of freedom allows rotation about the span of the wing while the chordwise motion is restrained. Therefore, torsion modes are not impacted by the changing hinge stiffness. The fold angle vs frequency plots in the section on the beam-rod wing modal analysis results demonstrate this. As hinge stiffness increases the characteristics demonstrated by the unfolded configuration bending modes become those demonstrated by more traditional wings. Increasing the hinge stiffness leads to a structure with less stiffness then that of the hinges so all wing bending takes place in the structure. At lower hinge stiffness values each of the joined sections remains rigid and bending takes place in the hinges. As the bending modes change frequency with changing hinge stiffness they interact with the torsion modes driving dynamic modal coalescence. In other words, flutter speed changes with changing wing fold angle and hinge stiffness. This phenomena is of particular concern if the stiffness provided by the actuator drops while motion takes place. Actuation systems which are not of the traditional hydraulic kind, but invoke thermal or other such similar properties may be of concern during vehicle configuration transition. In this case limitations would be placed on the vehicle addressing morphing flight conditions.

Another interesting observation is the crossing of the modes seen in the modal analysis which leads to flutter mechanism switching. In both models analyzed the change in flutter mechanism is tied to the interaction of the modes which vary during wing folding. Once again the beam-rod wing demonstrates this as it is seen the flutter mechanism changes occur as the modes begin to interact. Up to that point flutter velocity is seen to decrease in a fairly linear fashion. Flutter velocity jumps quite significantly following the modal interaction. The built-up FEM model demonstrates changing flutter mechanisms and velocities at each fold angle and hinge stiffness analyzed. Once again this is of particular concern if the stiffness provided by the actuation system is dynamic. Vehicle weight also plays a significant role in the flutter mode. In the case of the built-up FEM wing, Table 1 shows body freedom flutter may be a concern as the vehicle approaches its empty weight. Flutter velocities are quite lower at this point as well. The drop in flutter velocity with decreasing weight is a classical result.

Future work in this area would involve tools which allow the modeling and analysis of this system to take place dynamically. As stated in the problem setup, quasi-steady motion was assumed and so these results are a "snapshot" of the true picture. However, the impact on flutter velocity and mechanism could be studied dynamically if one analyzes the vehicle while the wings are changing configuration, both folding and unfolding. In this case, flutter results would not only be a function of wing hinge stiffness and fold angle but fold rate as well, allowing better understanding of the flutter problem in its entirety. Another future analysis would involve development of an optimization tool which would allow optimization of multiple constraints over multiple air loads involving multiple structural configurations.

The work done to date has shown the importance of the continuous development and use of advanced structural analysis tools. Aircraft continue to grow in complexity and capability and these tools will be essential to the successful implementation of radical flight altering concepts.

References

[1] Pace, S., "Valkyrie: North American XB-70," *TAB Books*, 2nd ed., Blue Ridge Summit, PA, 1990, chap. 3.

[2] Pitt, D. M., "Static and Dynamic Aeroelastic Analysis of Structural Wing Fold Hinges That are Employed as an Aeroelastic Tailoring Tool," *45th AIAA/ASME/ASCE /AHS/ASC Structures, Structural Dynamics & Materials Conference*, Palm Springs, California, 19–22 April 2004.

[3] Livne, Eli., "Future of Airplane Aeroelasticity," *Journal of Aircraft*, Vol. 40, No. 6, 2003, pp. 1066–1092. doi:10.2514/2.7218

[4] Snyder, M., Sanders, B., Frank, G., and Eastep, F., "Vibration and Flutter Characteristics of a Folding Wing," *46th AIAA/ASME/ASCE / AHS/ASC Structures, Structural Dynamics & Materials Conference*, Austin, Texas, 18–21 April 2005.

[5] Snyder, M., Sanders, B., Frank, G., and Eastep, F., "Sensitivity of Flutter to Fold Orientation and Spring Stiffness of a Simple Folding Wing," *International Forum on Aeroelasticity and Structural Dynamics 2005*, Munich, Germany, 28 June–1 July 2005.

[6] Goland, M., "The Flutter of a Uniform Cantilever Wing," *Journal of Applied Mechanics*, Vol. 12, No. 4, Dec. 1945.

[7] Arnaiz, H. H., Peterson, J. B., and Daugherty, J. C., "Wind-Tunnel/ Flight Correlation Study of Aerodynamic Characterisitcs of a Large Flexible Supersonic Cruise Airplane (XB-70-1)," NASA Technical Paper 1516, March 1980.

[8] Love, H. H., Zink, P. S., Stroud, R. L., Bye, D. R., and Chase, C., "Impact of Actuation Concepts on Morphing Aircraft Structures," *45th AIAA/ASME/ASCE /AHS/ASC Structures, Structural Dynamics & Materials Conference*, Palm Springs, California, 19–22 April 2004.